

IACS/2021/04/05

Computing quivers for two and higher loops for the colored planar ϕ^3 theory

Prafulla Oak*

Indian Association for the Cultivation of Sciences
2A and 2B Raja S.C. Mullick road, Kolkata-700032
India

Abstract

We introduce Feynman-like rules to compute quivers for two loops and higher for the coloured planar ϕ^3 theory for winding number zero. We demonstrate this for a few cases.

Contents

1	Introduction	3
2	A quick review of the "Amplituhedron" formalism for scalar theories	4
2.1	Kinematic space	4
2.2	Planar kinematic variables and the scattering form.	5
2.3	The kinematic associahedron.	8

*prafullaoakwork@gmail.com

3	Known results of quivers for tree level and 1-loop processes	10
3.1	Tree level	10
3.2	All unique 1-loop processes	11
4	Construction of quivers from Feynman diagrams	13
4.1	Feynman diagram-like rules for writing down quivers from Feynman diagrams	13
4.2	Tree level diagrams	16
4.3	1-loop diagrams	17
5	Examples of quivers for two and three loop processes.	21
5.1	2-loop diagrams	21
5.2	Some non-trivial cases for 3-loop diagrams	26
5.3	Generalization to all loop order and any particle number	29
6	Summary and Conclusions	29

1 Introduction

Scattering amplitudes are the most basic observables in physics. Also, they are the only known observable of quantum gravity in asymptotically flat space-time. The scattering amplitudes, in the case of AdS spaces, are easily calculable, as all the in and out states are observables of the local theory of the boundary, which for the AdS case, is the local quantum field theory in flat space. This question is very hard to answer in bulk flat space-time, the reason being that we do not have a good answer to what the theory at infinity should be in this case. The initial S-matrix theorists were looking for a first principle derivation of the fundamental analyticity properties encoding unitarity and causality in the S-matrix, and in this way to find the principles for the theory of S-matrix. This approach did not succeed and a new strategy was needed to address this problem. The modern strategy is to look for new principles and laws, which one expects, to be associated with entirely new mathematical structures, that produce the S-matrix as the answer to an entirely different class of questions and see unitarity and causality as emerging from them rather than being imposed a priori. This approach was initially taken by [1] to analyse scattering amplitudes in super-symmetric quantum field theories. They later extended it to a class of non-super-symmetric coloured scalar ϕ^3 theories [2]. They started by introducing a planar scattering form, which is a differential form on the space of kinematic variables, that encodes information about on-shell tree level scattering amplitudes, thus "upgrading" amplitudes to forms. Further, a precise connection was established between this scattering form and a polytope known as the "Associahedron". This connection leads one precisely to a new understanding of locality and unitarity as emergent properties from the combinatorial and geometric properties of the polytopes, as one had hoped for in the beginning. To obtain these forms one looks at the duals to the Feynman diagram, as will be shown later, and then triangulates them. One can associate quivers to these triangulations. We will show this in one of the sections. The quivers for tree level processes were shown to be A_n Dynkin type quivers. Similarly, the quivers for 1-loop processes were shown to be of the D_n type Dynkin quivers [10]. Some of these were demonstrated by [8] and there were unique such quivers for tree level and 1-loop level processes. For higher loops the association of Dynkin-type quivers with loop order breaks down. For 2-loops and higher there were problems with non-uniqueness of the quivers as described by [8], that, one could associate many quivers to a process, as there were many triangulations one could associate to each Feynman diagram. This happens because the winding number of the diagonals is undetermined and that leads to there being a non-unique set of triangulations.

A lot of progress has been made in this area parallelly. Much work has been done on effective field theories [11, 19]. It has also been shown that the Yangian symmetry is manifest in this approach [1, 3, 4]. It was shown in [2] that the CHY

formula gives scattering amplitude for a large class of theories as integrals of world sheet moduli space. It has been known for sometime that the compactification of this moduli space is an associahedron [39, 40] and in [2] it was shown that this worldsheet associahedron is diffeomorphic to the associahedron sitting inside the kinematic space. Scattering equations, which are the basic building blocks of the CHY formula, are precisely these diffeomorphisms. It naturally follows, that the CHY integrand for the ϕ^3 theory is a pullback of the canonical form on the associahedron.

In this paper we propose a way to construct the quivers corresponding to each Feynman diagram at winding number zero. We do not know the answers for higher winding numbers or any consequences thereof, but nonetheless this seems like an interesting heuristic exercise to carry out. In section 2, we will give a very quick review of the "Amplituhedron" program for the coloured scalar ϕ^3 theory. Then in section 3 we will briefly mention the known quivers for tree level and 1-loop processes. In the next section we motivate and prescribe a set of Feynman-like rules to construct quivers from Feynman diagrams directly. In section 5 we demonstrate the construction of quivers for 2-loop and 3-loop processes. In section 6 we give a brief summary of the results obtained.

2 A quick review of the "Amplituhedron" formalism for scalar theories

In this section we summarize the results of [2].

2.1 Kinematic space

The Kinematic space \mathcal{K}_n of n massless momenta p_i , $i=1,\dots,n$, is spanned by nC_2 number of Mandelstam variables,

$$s_{ij} = (p_i + p_j)^2 = 2p_i \cdot p_j \quad (2.1.1)$$

For space-time dimensions $d < n - 1$, all of them are not linearly independent and they are constrained by

$$\sum_{j=1; j \neq i} s_{ij} = 0, \quad i = 1, \dots, n \quad (2.1.2)$$

Therefore the dimension of \mathcal{K}_n reduces to

$$\dim(\mathcal{K}_n) = {}^nC_2 - n = \frac{n(n-3)}{2} \quad (2.1.3)$$

For any set of particle labels

$$I \subset \{1, \dots, n\} \quad (2.1.4)$$

one can define Mandelstamm variables as follows,

$$s_I = (\sum_{i \in I} p_i)^2 = \sum_{i, j \in I; i < j} s_{ij} \quad (2.1.5)$$

2.2 Planar kinematic variables and the scattering form.

We always order the particles cyclically and define planar kinematic variables,

$$X_{i,j} = s_{i,i+1,\dots,j-1}; \quad 1 \leq i < j \leq n \quad (2.2.6)$$

Here

$$s_{i,i+1,\dots,j-1} = (p_i + p_{i+1} + \dots + p_{j-1})^2 = 2(p_i \cdot p_{i+1} + \dots + p_{j-2} \cdot p_{j-1}) \quad (2.2.7)$$

Then $X_{i,i+1} = X_{1,n} = 0$. The variables $X_{i,j}$ can be visualized as the diagonals between the i^{th} and j^{th} vertices of the corresponding n -gon. (See figure.)

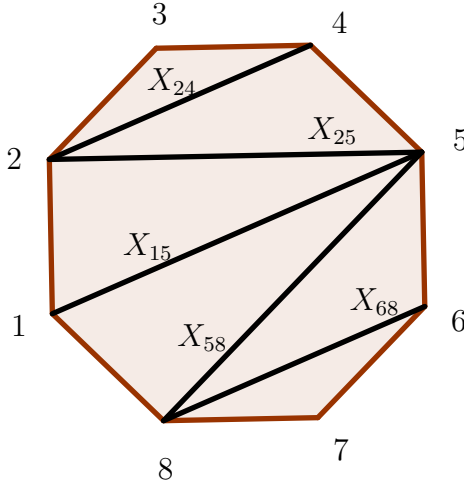


Figure 1: Fully triangulated octagon. The X_{ij} are the diagonals.

These variables are related to the Mandelstam variables by the following relation

$$s_{ij} = X_{i,j+1} + X_{i+1,j} - X_{i,j} - X_{i+1,j+1} \quad (2.2.8)$$

In other words $X_{i,j}$'s are dual to $\frac{n(n-3)}{2}$ diagonals of an n -gon made up of edges with momenta p_1, \dots, p_n . Each diagonal i.e., X_{ij} cuts the internal propagator of a

Feynman diagram once. Thus there exists a one-one correspondence between cuts of cubic graphs and complete triangulations of an n -gon.

A partial triangulation of a regular n -gon is a set of non-crossing diagonals which do not divide the n -gon into $(n-2)$ triangles.

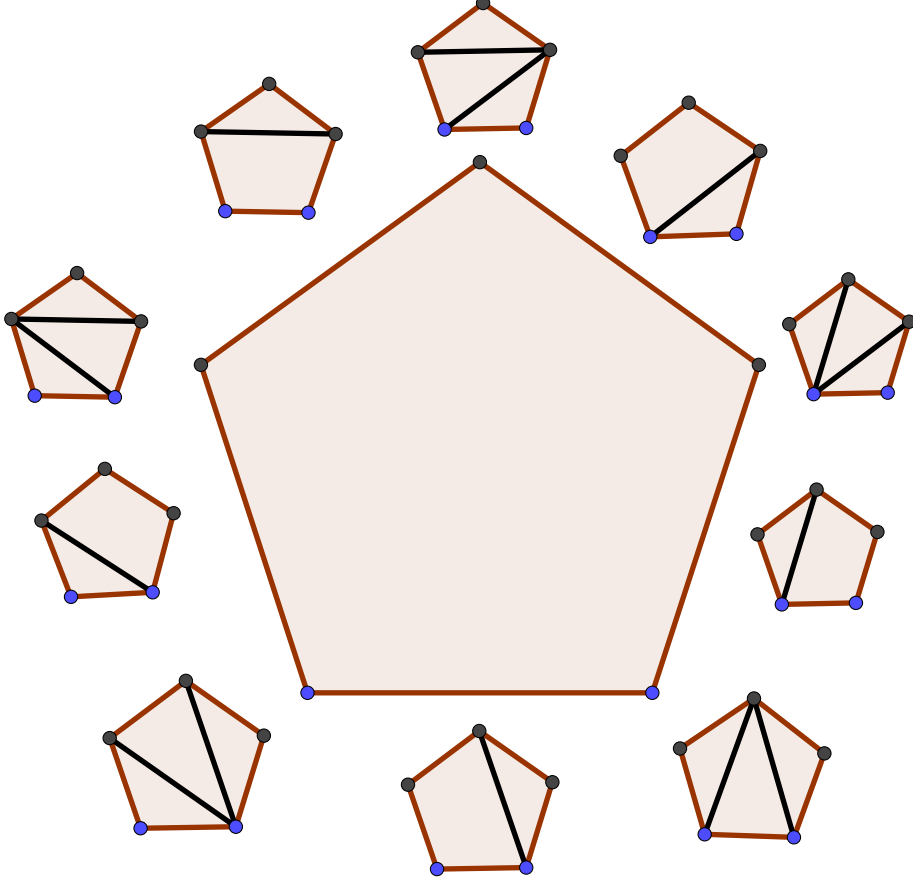


Figure 2: The 2-dimensional associahedron \mathcal{A}_5 5 partial triangulations represented by 5 diagonals on co-dim 1 faces. 5 complete triangulations represented by 5 vertices on co-dim 0 vertices.

The associahedron of dimension $(n-3)$ is a polytope whose co-dimension d boundaries are in one-to-one correspondence with partial triangulations by d diagonals. The vertices represent complete triangulations and the k -faces represent k partial triangulations of the n -gon. The total number of ways to triangulate a convex n -gon by non-intersecting diagonals is the $(n-2)$ -eth Catalan number, $C_{n-2} = \frac{1}{n-1} {}^{2n-4}C_{n-2}$. We refer the reader to [2] for further details.

We now define the planar scattering form. It is a differential form on the space of kinematic variables X_{ij} that encodes information about on-shell tree-level

scattering amplitudes of the scalar ϕ^3 theory. Let g denote a tree cubic graph with propagators $X_{i_a j_a}$ for $a = 1, \dots, n-3$. For each ordering of these propagators, we assign a value $\text{sign}(g) \in \pm$ to the graph with the property that flipping two propagators flips the sign. The form must have logarithmic singularities at $X_{i_a j_a} = 0$. Therefore one assigns to the graph a $d \log$ form and thus defines the planar scattering form of rank $(n-3)$:

$$\Omega_n^{n-3} := \sum_{\text{planar } g} \text{sign}(g) \wedge_{a=1}^{n-3} d \log X_{i_a j_a} \quad (2.2.9)$$

where the sum is over each planar cubic graph g . There are two sign choices for each graph, therefore there are many different scattering forms. One can fix the scattering form uniquely if one demands projectivity of the differential form, i.e. if one requires that the form should be invariant under local $GL(1)$ transformations $X_{ij} \rightarrow \Lambda(X) X_{ij}$ for any index pair (i,j) . We use projectivity to define an operation called mutation. Two planar sub-graphs g and g' are related by a mutation if we can obtain one from the other just by exchanging 4-point sub-graph channels, figure 3. As we can see X_{ij} and $X_{i'j'}$ are the mutated propagators of graphs g and g' respectively. Let's denote the rest of the common propagators as $X_{i_b j_b}$ with $b = 1, \dots, n-4$. Under $X_{ij} \rightarrow \Lambda(X) X_{ij}$ the scattering form becomes,

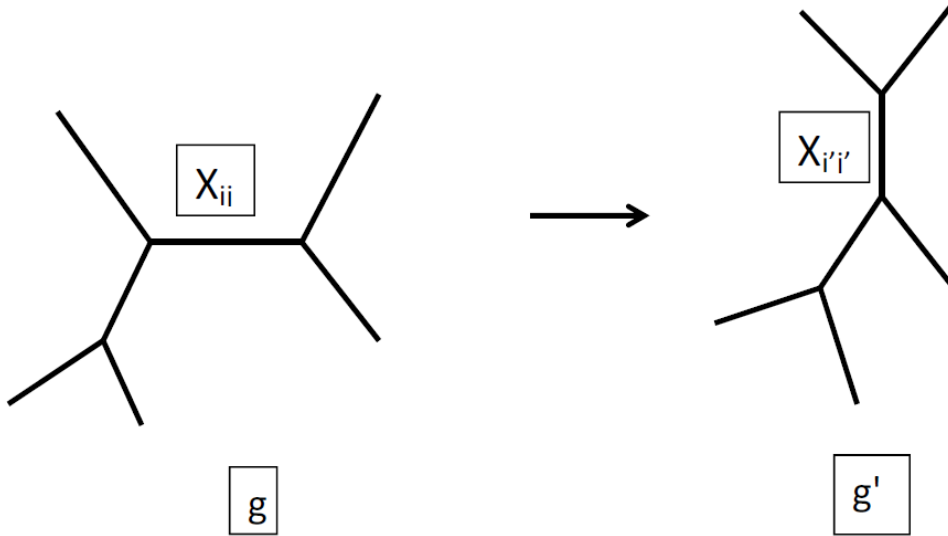


Figure 3: Two graphs related by a mutation given by an exchange of $X_{ij} \rightarrow X_{i'j'}$ in a 4-point sub-graph.

$$\text{sign}(g) d \log(\Lambda(X) X_{ij}) \wedge_{b=1}^{n-4} d \log X_{i_b j_b} + \dots \quad (2.2.10)$$

$$\text{sign}(g') \, d\log(\Lambda(X)X_{i'j'})\Lambda_{b=1}^{n-4} \, d\log X_{ibjb} + \dots \quad (2.2.11)$$

Collecting the $d\log\Lambda$ terms

$$\text{sign}(g) \, d\log\Lambda(X)\Lambda_{b=1}^{n-4} \, d\log X_{ibjb} + \text{sign}(g') \, d\log\Lambda(X)\Lambda_{b=1}^{n-4} \, d\log X_{ibjb} \quad (2.2.12)$$

$$= (\text{sign}(g) + \text{sign}(g')) \, d\log(\Lambda(X)X_{ij})\Lambda_{b=1}^{n-4} \, d\log X_{ibjb} \quad (2.2.13)$$

Since we demand projectivity, the $\Lambda(X)$ dependence has to disappear, i.e. when

$$\text{sign}(g) = -\text{sign}(g') \quad (2.2.14)$$

for each mutation.

2.3 The kinematic associahedron.

We described above how one gets an associahedron \mathcal{A}_n inside the kinematic space \mathcal{K}_n but it is not evident how it should be embedded in \mathcal{K}_n . Because \mathcal{A}_n and \mathcal{K}_n are of different dimensionality, $\dim(\mathcal{A}_n) = (n-3)$ and $\dim(\mathcal{K}_n) = \frac{n(n-3)}{2}$ respectively, we have to impose constraints to embed \mathcal{A}_n inside \mathcal{K}_n . One natural choice is to demand all planar kinematic variables being positive,

$$X_{ij} \geq; \quad 1 \leq i < j \leq n. \quad (2.3.15)$$

These are $\frac{n(n-3)}{2}$ inequalities and thus cut out a big simplex Δ_n inside \mathcal{K}_n which is still $\frac{n(n-3)}{2}$ dimensional. Therefore we need $\frac{n(n-3)}{2} - n - 3 = \frac{(n-2)(n-3)}{2}$ more constraints to embed \mathcal{A}_n inside \mathcal{K}_n . To do that we impose the following constraints,

$$s_{ij} = -c_{ij}; \quad 1 \leq i < j \leq n-1, \quad |i-j| \geq 2 \quad (2.3.16)$$

where c_{ij} are positive constraints.

These constraints give a space \mathcal{H}_n of dimension $(n-3)$ which is precisely the dimension of \mathcal{A}_n . The kinematic associahedron \mathcal{A}_n can now be embedded in \mathcal{K}_n as the intersection of the simplex Δ_n and the subspace \mathcal{H}_n as follows,

$$\mathcal{A}_n := \mathcal{H}_n \cap \Delta_n. \quad (2.3.17)$$

Once one has the associahedron in \mathcal{K}_n all one has to do is to obtain its canonical form $\Omega(\mathcal{A}_n)$.

Since an associahedron is a simple polytope one can directly write down its canonical form as follows,

$$\Omega(\mathcal{A}_n) = \sum_{\text{vertex } Z} \text{sign}(Z) \Lambda_{a=1}^{n-3} d \log X_{i_a j_a} \quad (2.3.18)$$

Here for each vertex Z , $X_{i_a j_a} = 0$ denote its adjacent facets for $a=1, \dots, n-3$. Now we claim that the above differential form 2.3.18 is identical to the pullback of the scattering form 2.2.9 in \mathcal{K}_n to the subspace \mathcal{H}_n . We can justify this statement by the identification $g \leftrightarrow Z$ and $\text{sign}(g) \leftrightarrow \text{sign}(Z)$.

1. There is a one to one correspondence between vertices Z and the planar cubic graphs g . Also, g and its corresponding vertex have the same propagators $X_{i_a j_a}$.
2. Let Z and Z' be two vertices related by mutation. Note that mutation can also be framed in the language of triangulation. Two triangulations are related by a mutation if one can be obtained from the other by exchanging exactly one diagonal. See figure 4.

Thus for Z and Z' vertices we have

$$\Lambda_{a=1}^{n-3} dX_{i_a j_a} = -\Lambda_{a=1}^{n-3} dX_{i'_a j'_a} \quad (2.3.19)$$

which leads to the sign-flip rule $\text{sign}(Z) = -\text{sign}(Z')$.

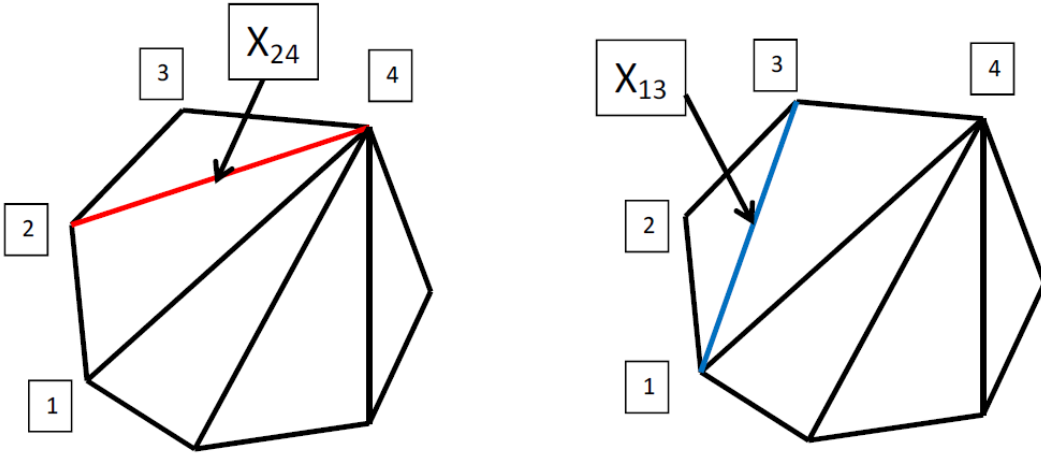


Figure 4: Two triangles related by a mutation $X_{24} \rightarrow X_{13}$.

Therefore one can construct the following quantity (an $(n-3)$ -form) which is independent of g on pullback.

$$d^{n-3}X := \text{sign}(g)\Lambda_{a=1}^{n-3}dX_{i_a j_a}. \quad (2.3.20)$$

Substituting this in 2.3.18 one gets,

$$\Omega(\mathcal{A}_n = \Sigma_{\text{planar } g} \frac{1}{\prod_{a=1}^{n-3} X_{i_a j_a}} d^{n-3}X. \quad (2.3.21)$$

Here

$$\mathcal{M}_n = \Sigma_{\text{planar } g} \frac{1}{\prod_{a=1}^{n-3} X_{i_a j_a}} \quad (2.3.22)$$

is the tree level n -point scattering amplitude for the cubic scalar theory.

3 Known results of quivers for tree level and 1-loop processes

In this section we review known results for tree level and 1-loop quivers.

3.1 Tree level

The quiver for the 4-point tree level scattering amplitude is given by a single node. As the number of particles increases, the number of internal lines also increases. The number of nodes of the quiver is determined by the number of internal lines. Thus for a 5-point scattering process, there are two internal lines, therefore two nodes, as shown in figure 5. Therefore for an n -point amplitude, there are $n - 1$ nodes in the quiver. Also, in the figure are the triangulations of the dual n -gons whose diagonals correspond to the internal lines and the quiver nodes. To get quivers from the triangulated diagrams, one associates circle shaped nodes to the diagonals, as shown. These are called unfrozen nodes. Also, we associate square shaped nodes to the external polygon. These are called frozen nodes. Now one connects all nodes without crossing any diagonals. This gives us the quiver for the particular triangulation.

In part 1 of figure 5, there are four frozen nodes and one unfrozen node. Thus we associate to this triangulation an A_1 type of Dynkin quiver. In part 2, there are two unfrozen nodes and connecting these gives us the A_2 type Dynkin quiver. In part 3, we have shown an A_{n-1} quiver, which corresponds to the $n - 1$ diagonals/unfrozen nodes of the triangulations.

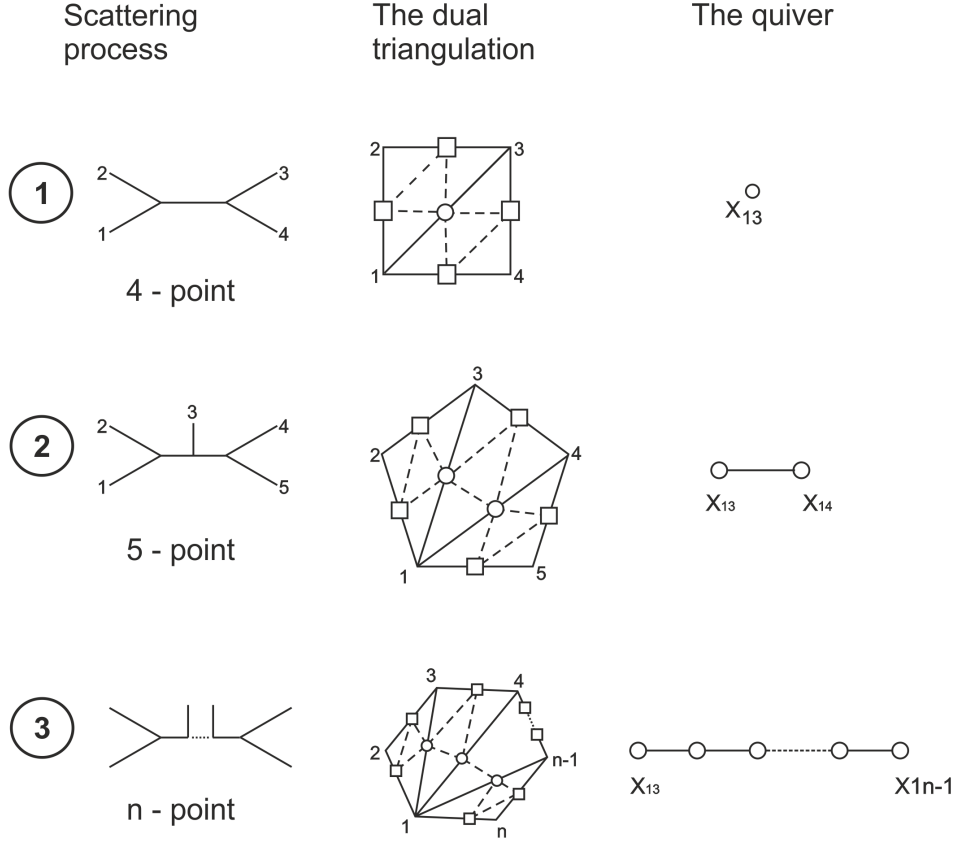


Figure 5: Demonstration of a few examples of quivers at tree level.

3.2 All unique 1-loop processes

In figure 6 we have tabulated 4-particle scattering processes with their dual n-gons (in this case, squares) triangulated and the associated quivers. We have only shown those processes which are unique upto permutations. Again as in the case of tree level diagrams one has to triangulate and mark the frozen and unfrozen nodes and connect them. An additional structure that is added to the polygon at 1-loop is the marked point in the middle of the diagram. This corresponds to the singularity of the loop. Thus for the case of 4-particles, we have a 4-gon, a square, with a marked point, and this has to be triangulated. This gives us four triangles with four unfrozen nodes and 4 diagonals. In part 1 and 2 we have shown the box diagram and the vertex corrections with their triangulations. We have also marked the frozen

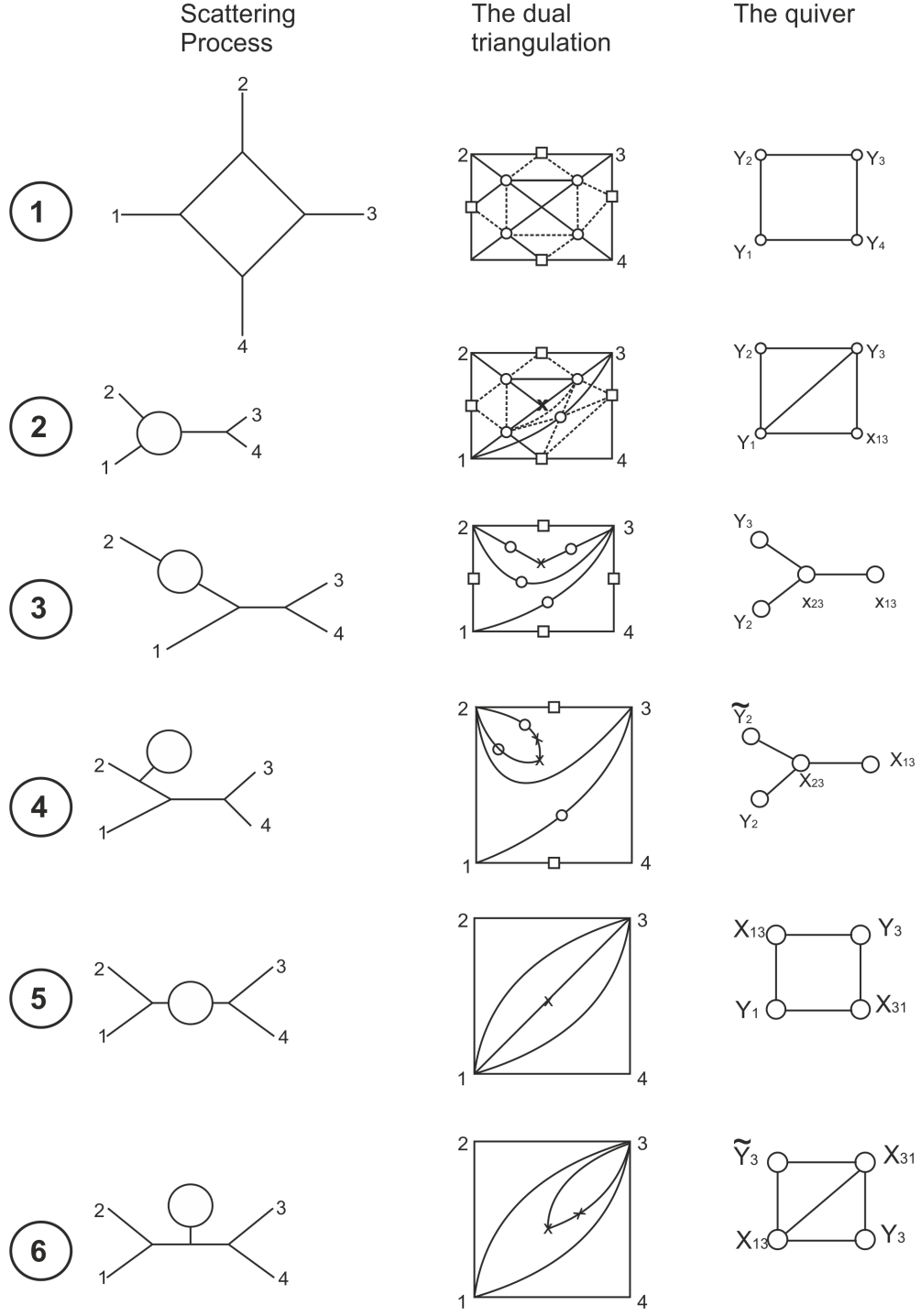


Figure 6: Quivers for ϕ^3 theories at 1-loop.

and the unfrozen nodes and connected them in the middle picture. Then we have shown the quiver by drawing the connected unfrozen nodes in the rightmost picture. The quivers, as can be seen, in this case are a square and a square with a diagonal. This is already a deviation from the association of D_4 Dynkin diagrams with the quivers. In parts 3 and 4 we have drawn the processes and only marked the frozen and unfrozen nodes. Then we have shown the quiver associated to it. It is however seen that it is only in these two cases that one gets to see the D_4 Dynkin diagrams.

In parts 5 and 6 we only show the processes, triangulations and the associated quivers. One can again see that the quivers in this case are a square and a square with a diagonal, not D_n type.

4 Construction of quivers from Feynman diagrams

We will discuss the rules for constructing quivers for ϕ^3 theory. These can be used to construct quivers at all loop orders at all particle numbers. We will also see examples in the following subsections upto 3-loops.

4.1 Feynman diagram-like rules for writing down quivers from Feynman diagrams

Rules:

1. Replace each internal line by a node as shown in the figure 7. Therefore the quiver of a 4-point scattering process is an A_1 quiver.
2. Associate a node to each internal line of a ϕ^3 vertex, then you connect two nodes along each "vertex line" as shown in the figure. Thus three nodes associated to the three lines of the ϕ^3 vertex have an associated quiver that is a triangle. (Ref. fig. 8).

We will append more rules to the list along the way.

Construction rule ①

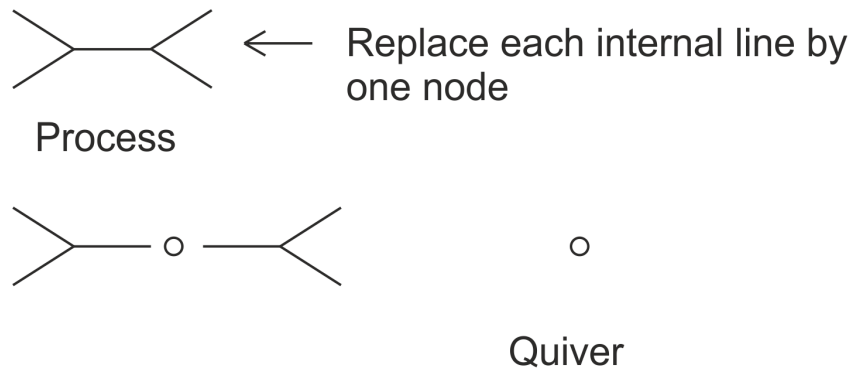


Figure 7: Construction rule 1.

Construction Rule ②

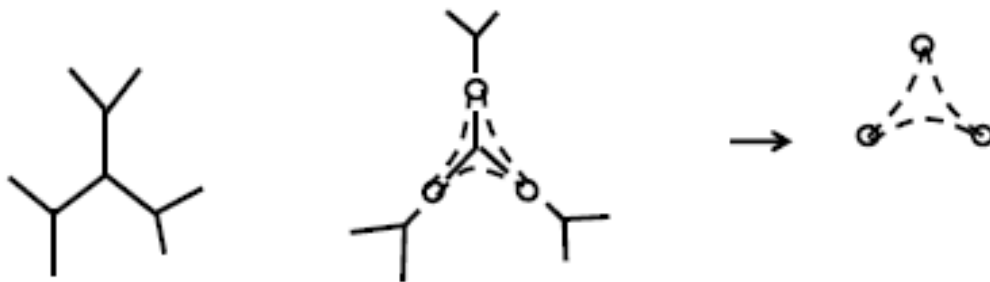


Figure 8: Construction rule 2.

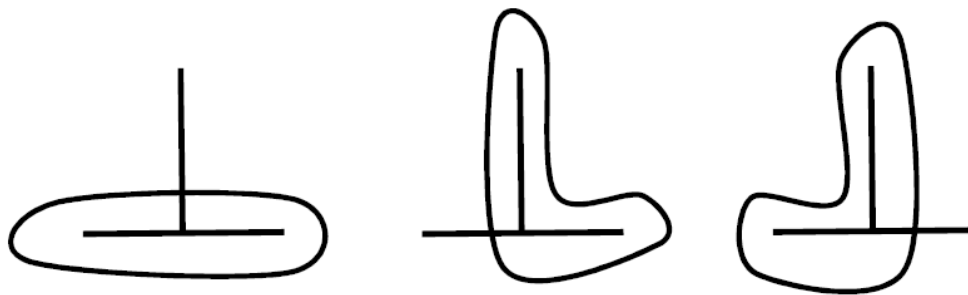


Figure 9: The three "vertex lines" of the ϕ^3 vertex.

4.2 Tree level diagrams

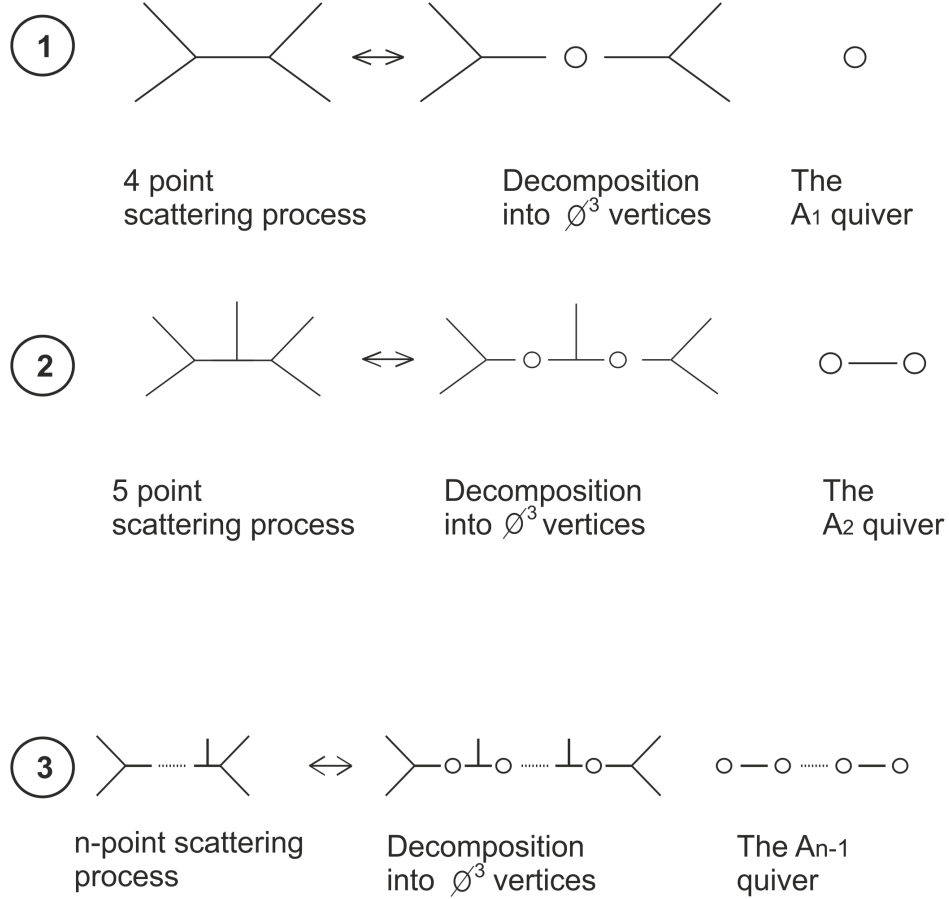


Figure 10: Construction of quivers for tree level processes.

At the tree level we have already seen the type of quivers one gets as one goes higher in particle numbers above, Fig. 5. We will show the construction of the quivers for the tree level processes for the 4,5 and the n particle cases, as we did above, using our technique.

For the 4 point case, there is a single internal line and therefore we get an A_1 quiver. For the 5-point there are two internal lines connected by one ϕ^3 vertex. We join the nodes across the "vertex lines". We get the A_2 quiver. For an n -point case we have $n - 1$ nodes connected by $n-2$ vertices. We connect all nodes all each vertex line and get the A_{n-1} quiver.

4.3 1-loop diagrams

Here we show the construction of the quivers for the 1-loop diagrams. In part 1 of the figure 11, we have the box diagram for a 4 particle scattering. In the next figure we decompose the diagram into its 3-point vertices as shown on the top right diagram. We associate nodes to all internal lines and connect the nodes across all "vertex lines". We do the same thing for diagram 2 in the figure. One can see in the bottom right diagram that there is an additional connection between nodes Y_1 and Y_3 , which is exactly what we saw in the construction of the quiver from the earlier method.

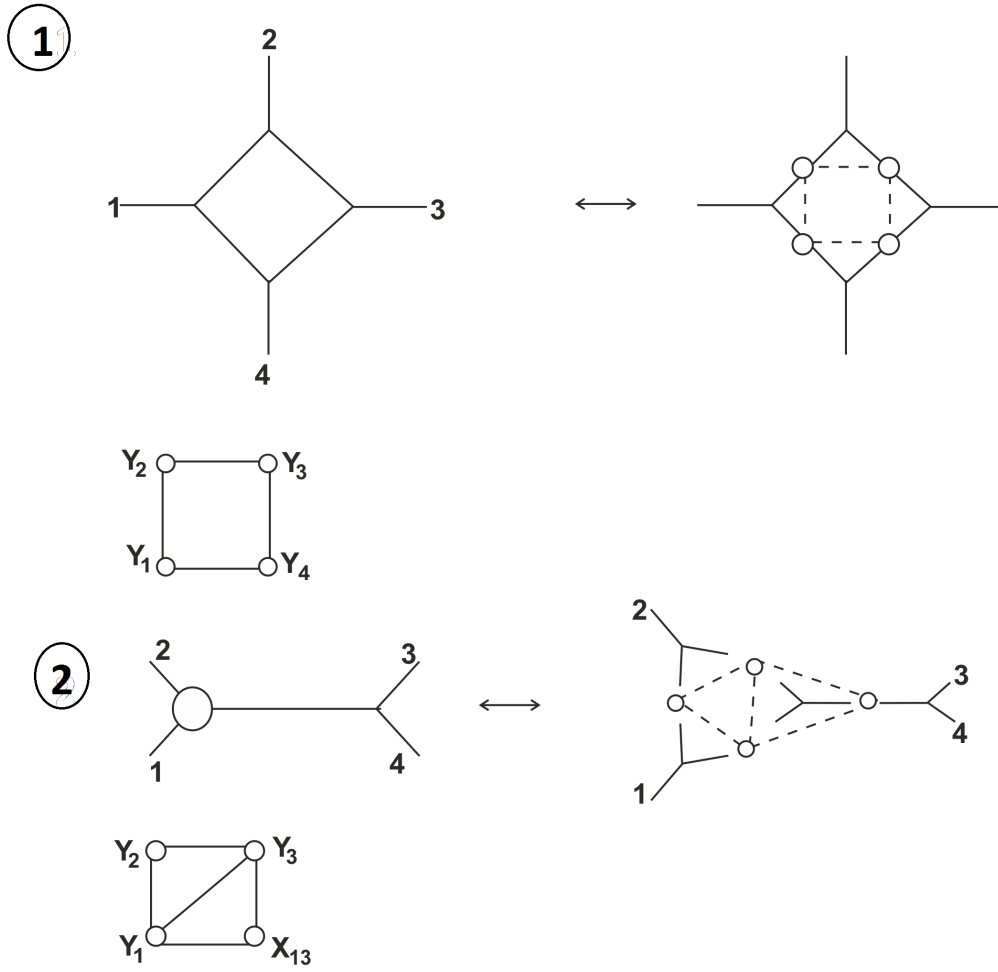


Figure 11: Construction of quivers for 4-point scattering processes at 1-loop

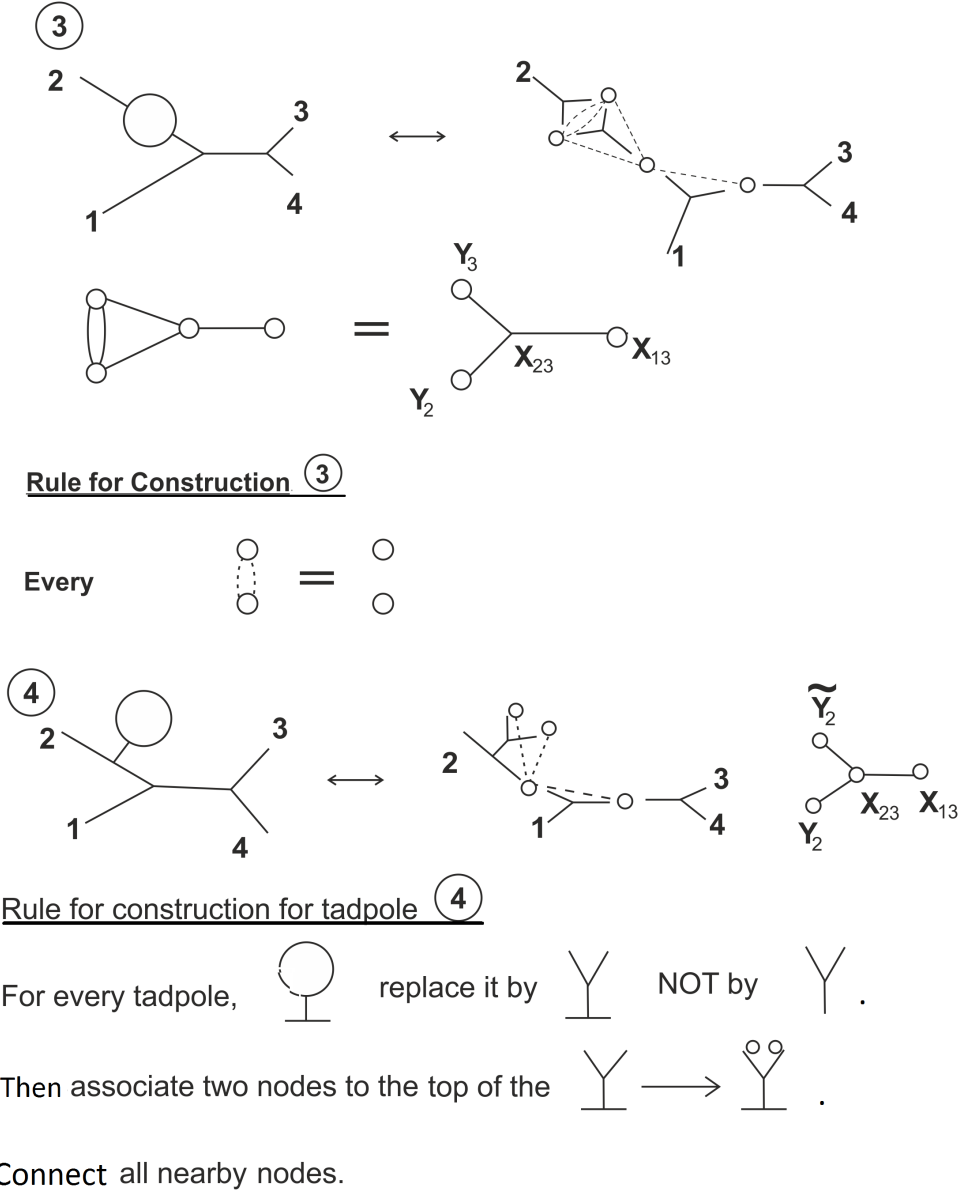


Figure 12: Construction rules 3 and 4.

In part 3 of figure 12, we can see that we come across a circular construction in one part of the quiver. This leads us to another rule,

Rule 3: Closed loops in quivers cancel out.

In part 4 of the figure we have a tadpole. We need another rule for this.

Rule 4:

For each tadpole with its base, replace it by a "Y" with its base, i.e. separate the tadpole from the rest of the diagram and cut its loop so that it becomes a "Y". Then associate two nodes to each of the open branches(two) of the "Y". Then we connect all nearby nodes with both these nodes.

In figure 13 part 5 we see another process. Here we again decompose the Feynman diagram of the process into its ϕ^3 vertices. We cancel out the circular part and we get the square quiver.

In part 6 we have a interesting example of a tadpole with internal lines on both sides. We again decompose the Feynman diagram into its vertices and associate two nodes with braches of the tadpole after cutting the loop open. Then, as mentioned before, we connect nodes on both sides of the tadpole to both nodes associated with the "Y" of the tadpole. This is exactly what we got for this process by connecting unfrozen nodes in 3.2. Thus we have shown that using our technique we can reproduce the quivers upto 1-loops. In the next section we will construct the quivers using our technique for 2-loops and show that it matches with the quivers obtained from the other technique upto winding number 0.

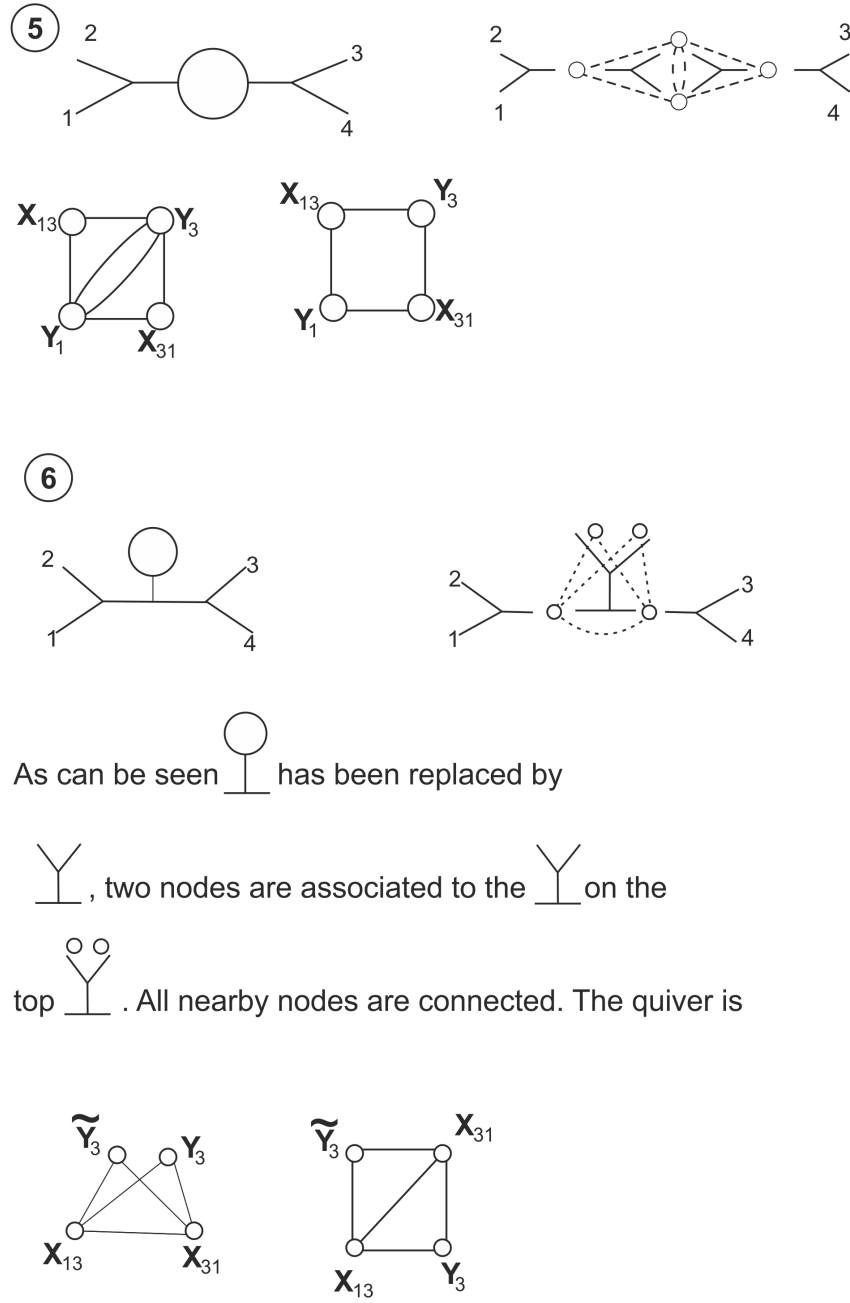


Figure 13: Number 5 is a demonstration of rule 3. Number 6 is a demonstration of rule 4.

5 Examples of quivers for two and three loop processes.

5.1 2-loop diagrams

Now we will construct the quiver for all unique 2-loop processes for 4 particles for the ϕ^3 theory. The quivers from triangulations for winding number zero can be easily obtained from known methods, just as in the case of the 1-loop processes which we will not show here.

In the figures we first show the process, then decompose the Feynman diagram into ϕ^3 vertices and tadpoles(ref. rule 4 above). Then we draw the quivers using the construction rules. As an example we will describe the first diagram, the rest are the same.

In part 1 of [14](#) we start with a diagram for two leg corrections. We decompose the Feynman diagram into the ϕ^3 vertices and assign nodes to the internal lines as described before. Then we connect all the nodes across each ϕ^3 "vertex line". This gives us the quiver. This matches exactly with quiver one gets from the previously known methods. We follow the same steps for the rest of the diagrams and if we draw the quiver from the known method upto winding number zero, then we will see that they all match exactly.

A few examples of two loop processes for ϕ^3

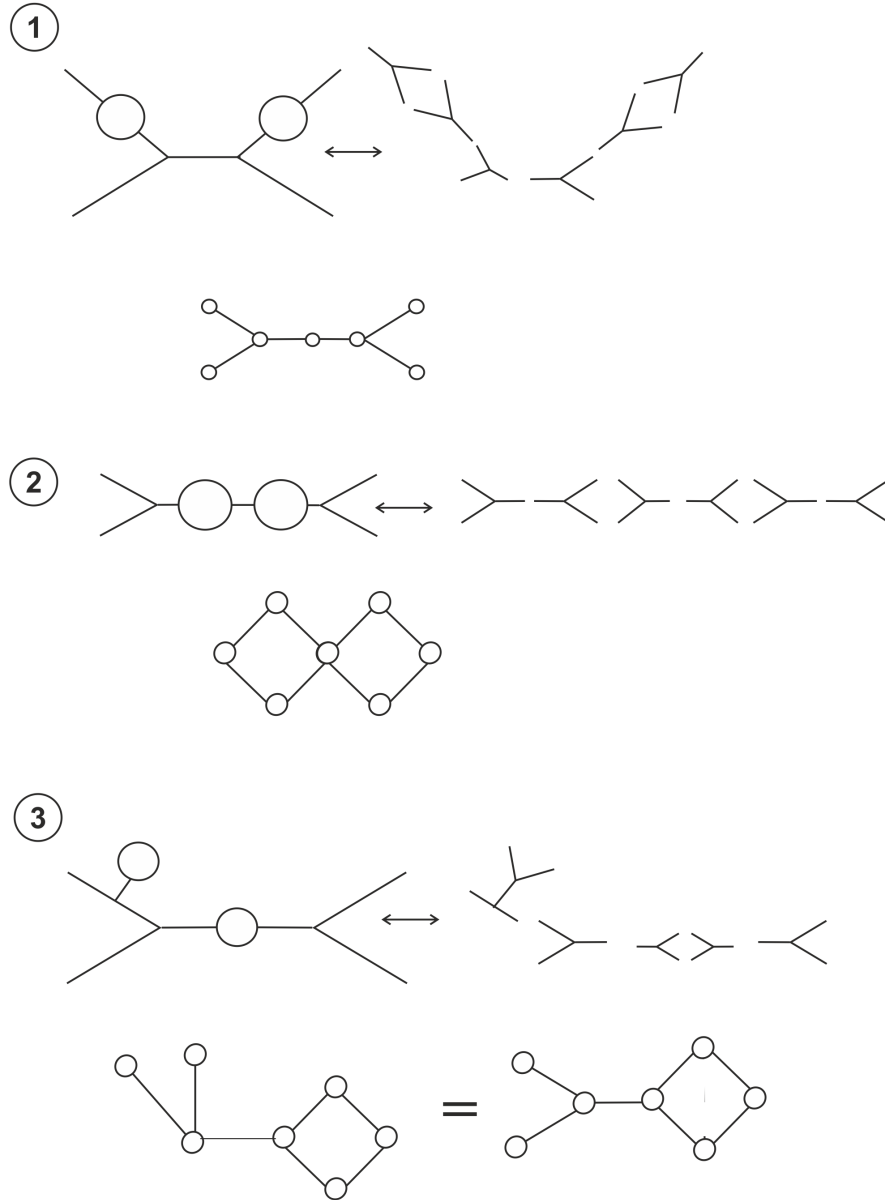


Figure 14: 2-loop processes for ϕ^3 .

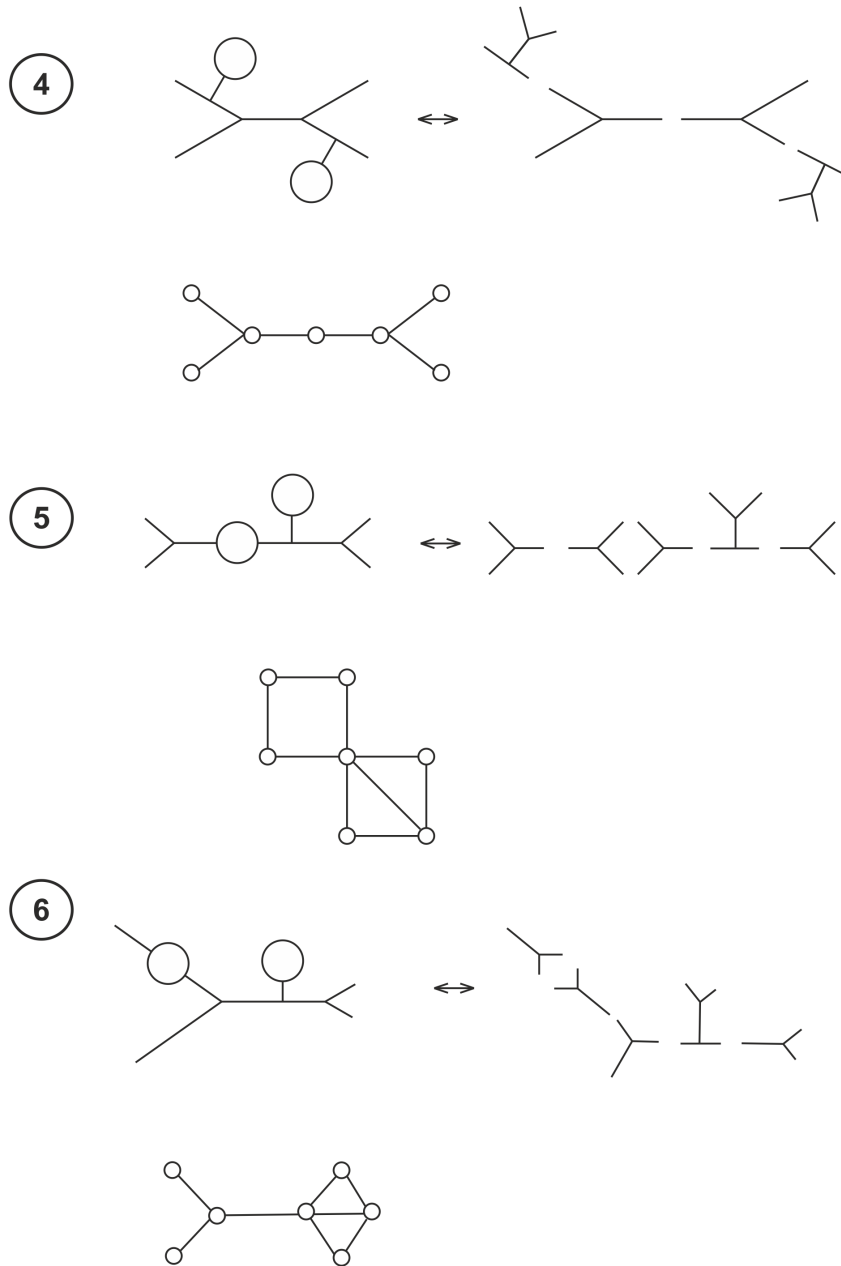


Figure 15: 2-loop processes for ϕ^3 .

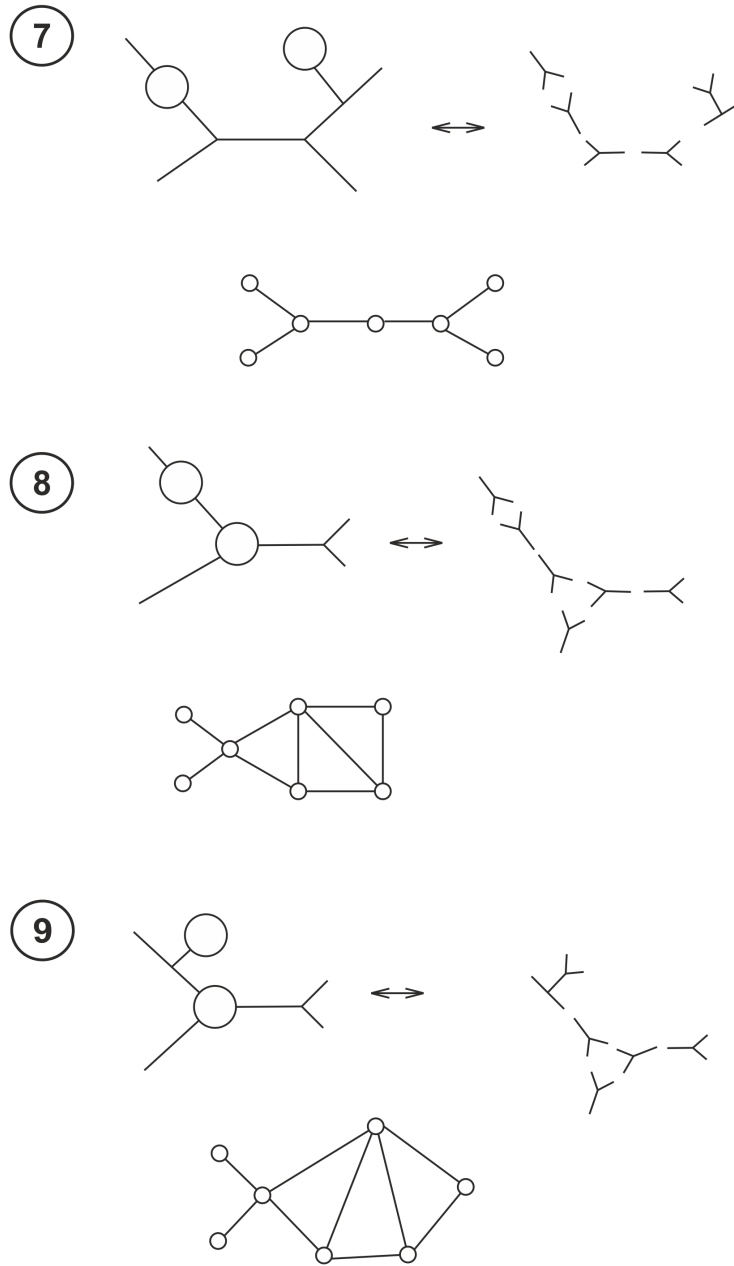


Figure 16: 2-loop processes for ϕ^3 .

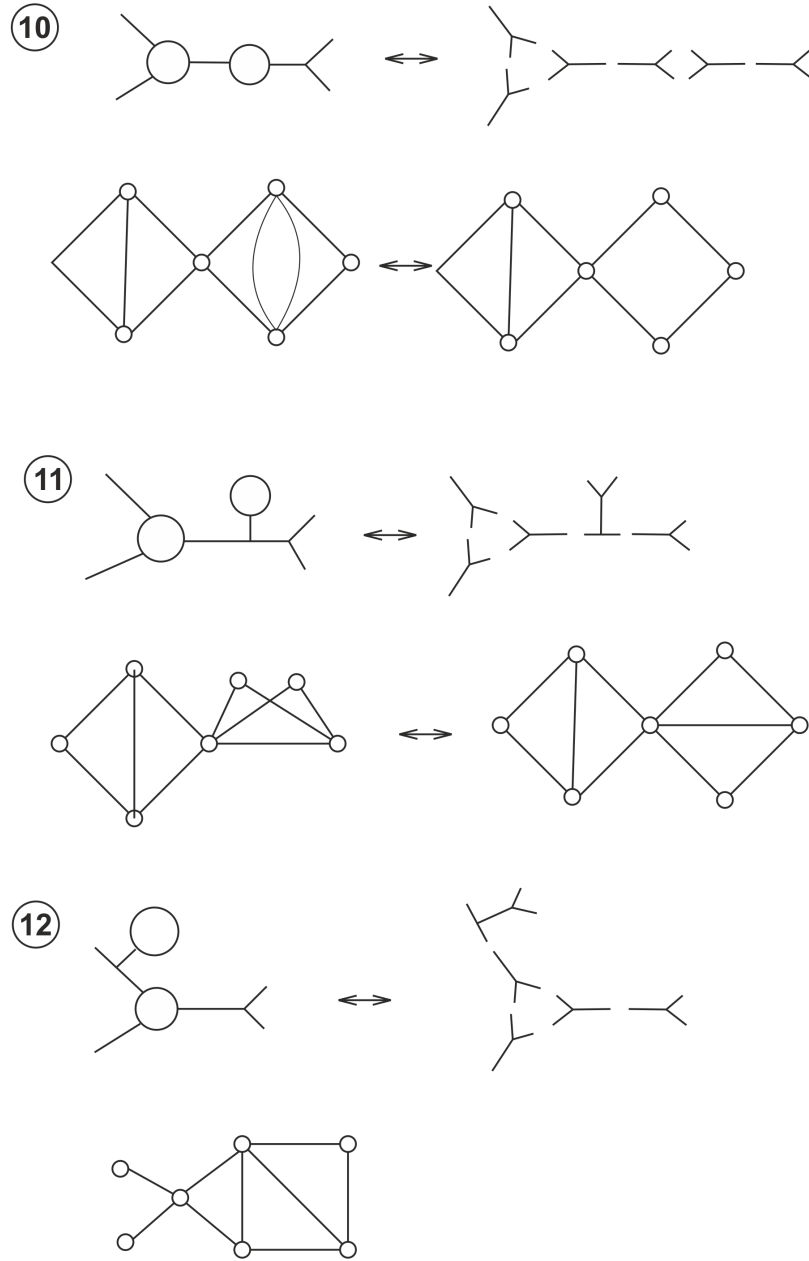


Figure 17: 2-loop processes for ϕ^3 .

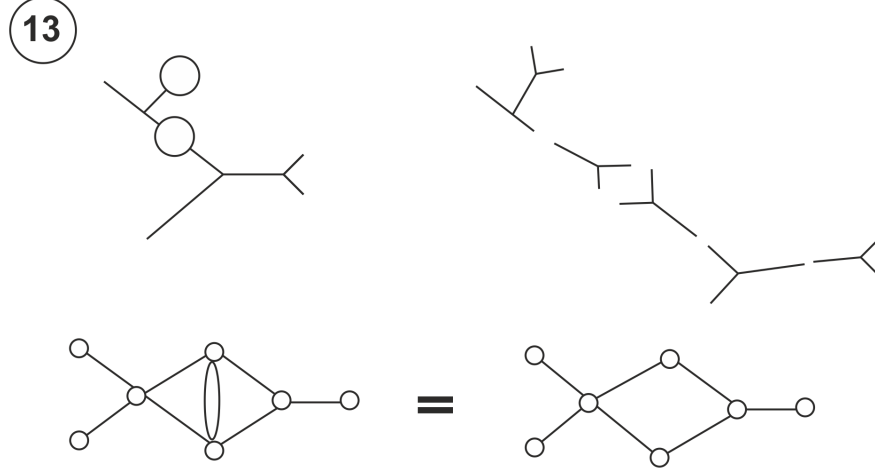


Figure 18: 2-loop processes for ϕ^3 .

5.2 Some non-trivial cases for 3-loop diagrams

Here we show two processes at 3-loops for 4 particle scattering for the ϕ^3 vertex. For both, we start with the process and then show the dual triangulation upto winding number zero with the frozen and unfrozen nodes indicated.

Next we construct the quiver using the usual method of connecting the nodes. Then we construct the quiver using our method and show that it matches with the one before.

We start with the scattering process. We triangulate the dual polygon. Then mark the unfrozen nodes and connect them so that no diagonal is crossed. This way only three nodes will always be connected. This connected picture is reproduced next and is the quiver upto winding number zero for this process. Next we decompose the Feynman diagram into ϕ^3 vertices and again assign nodes to the internal lines. Then we connect across all vertex lines. This gives us a quiver drawn on the bottom right. This matches exactly with the quiver we drew from the previous method.

We follow exactly the same steps for the next case and we again see that the quiver from our technique exactly matches the quiver from the previously known method.

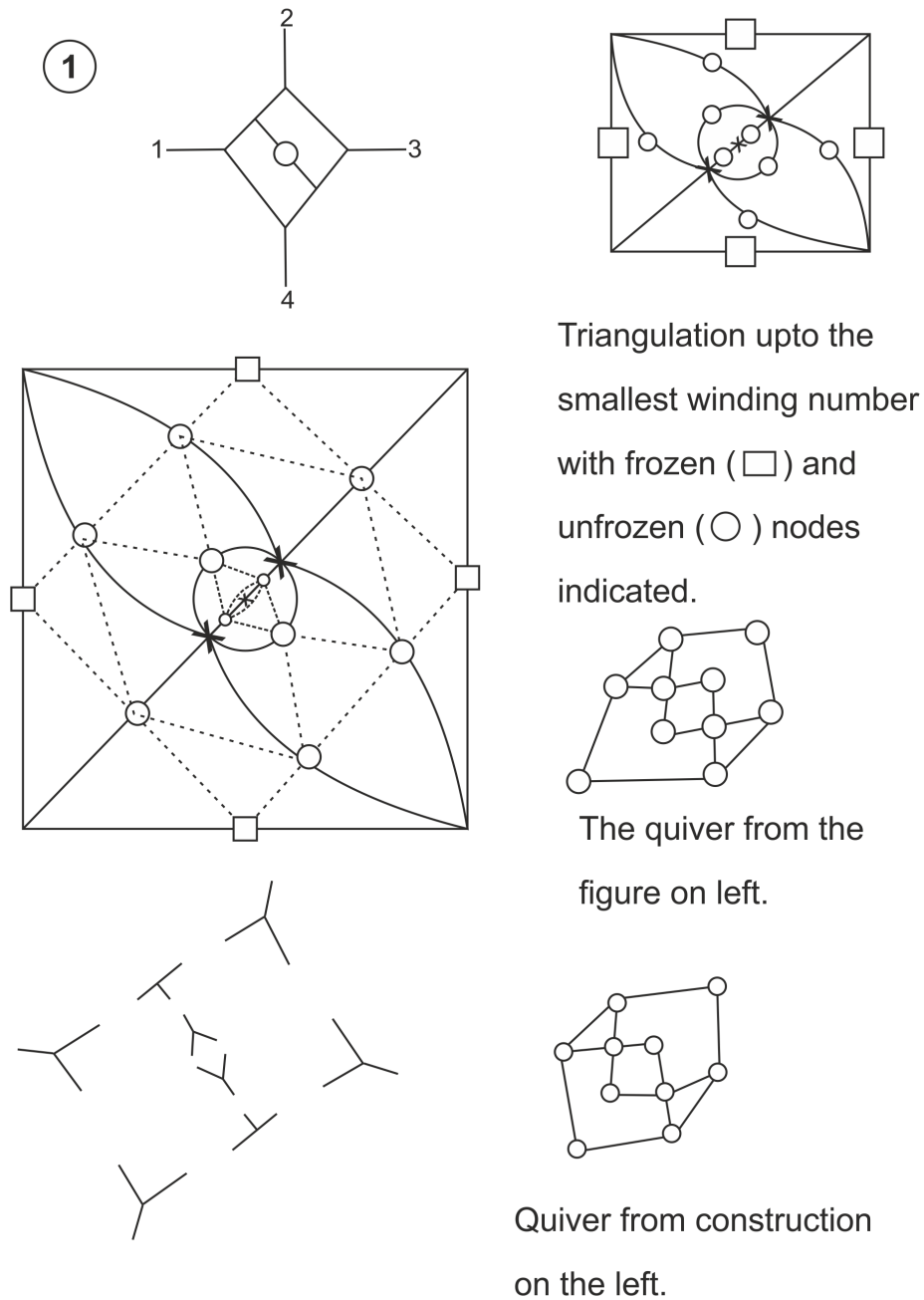
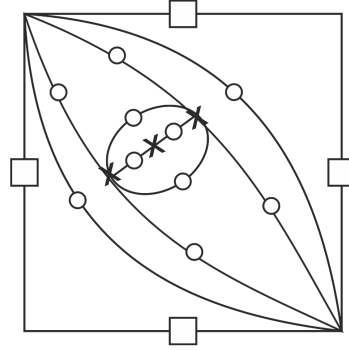
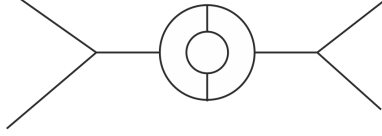


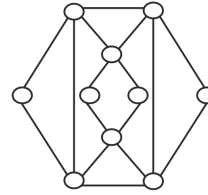
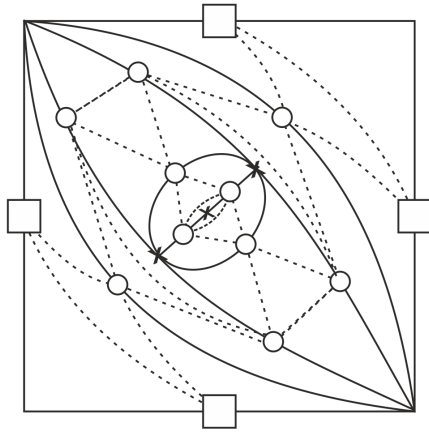
Figure 19: 3-loop processes for ϕ^3 theories.

①

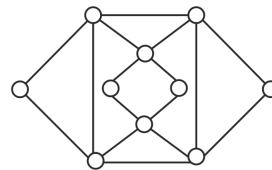
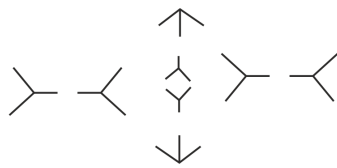


Triangulation upto the
smallest winding number.

All nodes indicated.



Quiver from triangulation.



Quiver from construction
on the left.

Figure 20: 3-loop processes for ϕ^3 theories.

5.3 Generalization to all loop order and any particle number

From the above examples it is clear that this program can give us quivers for any loop order for ϕ^3 theory for any number of particles for winding number zero.

6 Summary and Conclusions

In this paper, we begin by explaining the need for the computation of the scattering amplitude of any process, namely, that they are the only observables of quantum gravity in asymptotically flat space-time. Then we explain the need of a new approach to the problem of computing scattering amplitudes, that, a first principles derivation of the fundamental analyticity properties encoding unitarity and causality of the theory of scattering amplitudes, failed. In the next section we introduce the "Amplituhedron" approach started by Nima Arkani-Hamed et al for coloured scalar theories. Then we expand on the problem of computing scattering amplitudes for these coloured scalar theories. In section 3 we review the known results for quivers for tree level and 1-loop cases. In section 4 we list the rules of construction of the quivers and construct quivers for the ϕ^3 theory to 3-loop order. It can be easily seen from here that this program can be generalized to all loop orders for any number of particles.

Future directions

We feel that extending this program to the case of ϕ^n theories for all loop orders, for any particle numbers would be a significant and an important step. We hope to address that in our next paper.

Acknowledgments

We are deeply indebted to Koushik Ray for the initial idea, extensive discussions and constant encouragement and guidance. This manuscript would not have been possible without him. We are also very grateful to Nima Arkani-Hamed for his extensive and enlightening set of lectures at the RDST school organized by ICTS, Bangalore.

References

- [1] N. Arkani-Hamed and J. Trnka, “The Amplituhedron,” JHEP **10**, 030 (2014) doi:10.1007/JHEP10(2014)030 [[arXiv:1312.2007](#) [hep-th]].
- [2] N. Arkani-Hamed, Y. Bai, S. He and G. Yan, “Scattering Forms and the Positive Geometry of Kinematics, Color and the Worldsheet,” JHEP **05**, 096 (2018) doi:10.1007/JHEP05(2018)096 [[arXiv:1711.09102](#) [hep-th]].
- [3] N. Arkani-Hamed, A. Hodges and J. Trnka, “Positive Amplitudes In The Amplituhedron,” JHEP **08**, 030 (2015) doi:10.1007/JHEP08(2015)030 [[arXiv:1412.8478](#) [hep-th]].
- [4] N. Arkani-Hamed and J. Trnka, “Into the Amplituhedron,” JHEP **12**, 182 (2014) doi:10.1007/JHEP12(2014)182 [[arXiv:1312.7878](#) [hep-th]].
- [5] N. Arkani-Hamed, J. L. Bourjaily, F. Cachazo, A. B. Goncharov, A. Postnikov and J. Trnka, “Grassmannian Geometry of Scattering Amplitudes,” doi:10.1017/CBO9781316091548 [[arXiv:1212.5605](#) [hep-th]].
- [6] N. Arkani-Hamed, L. Rodina and J. Trnka, “Locality and Unitarity of Scattering Amplitudes from Singularities and Gauge Invariance,” Phys. Rev. Lett. **120**, no.23, 231602 (2018) doi:10.1103/PhysRevLett.120.231602 [[arXiv:1612.02797](#) [hep-th]].
- [7] N. Arkani-Hamed, Y. Bai and T. Lam, “Positive Geometries and Canonical Forms,” JHEP **11**, 039 (2017) doi:10.1007/JHEP11(2017)039 [[arXiv:1703.04541](#) [hep-th]].
- [8] School on Recent Developments in S-matrix theories(online), August 2020, ICTS, Bangalore.
- [9] N. Arkani-Hamed, S. He and T. Lam, “Stringy canonical forms,” JHEP **02**, 069 (2021) doi:10.1007/JHEP02(2021)069 [[arXiv:1912.08707](#) [hep-th]].
- [10] N. Arkani-Hamed, S. He, G. Salvatori and H. Thomas, “Causal Diamonds, Cluster Polytopes and Scattering Amplitudes,” [[arXiv:1912.12948](#) [hep-th]].
- [11] N. Arkani-Hamed, T. C. Huang and Y. T. Huang, “The EFT-Hedron,” [[arXiv:2012.15849](#) [hep-th]].
- [12] N. Arkani-Hamed, S. He and T. Lam, “Cluster configuration spaces of finite type,” [[arXiv:2005.11419](#) [math.AG]].

- [13] S. He and Z. Li, “A note on letters of Yangian invariants,” JHEP **02**, 155 (2021) doi:10.1007/JHEP02(2021)155 [[arXiv:2007.01574](#) [hep-th]].
- [14] S. He, Z. Li, P. Raman and C. Zhang, “Stringy canonical forms and binary geometries from associahedra, cyclohedra and generalized permutohedra,” JHEP **10**, 054 (2020) doi:10.1007/JHEP10(2020)054 [[arXiv:2005.07395](#) [hep-th]].
- [15] S. He, L. Hou, J. Tian and Y. Zhang, “Kinematic numerators from the world-sheet: cubic trees from labelled trees,” [[arXiv:2103.15810](#) [hep-th]].
- [16] S. He, Z. Li and Q. Yang, “Notes on cluster algebras and some all-loop Feynman integrals,” [[arXiv:2103.02796](#) [hep-th]].
- [17] S. He, Z. Li, Q. Yang and C. Zhang, “Feynman Integrals and Scattering Amplitudes from Wilson Loops,” [[arXiv:2012.15042](#) [hep-th]].
- [18] S. He, Z. Li, Y. Tang and Q. Yang, “The Wilson-loop $d\log$ representation for Feynman integrals,” [[arXiv:2012.13094](#) [hep-th]].
- [19] C. Cheung, K. Kampf, J. Novotny, C. H. Shen and J. Trnka, “A Periodic Table of Effective Field Theories,” JHEP **02**, 020 (2017) doi:10.1007/JHEP02(2017)020 [[arXiv:1611.03137](#) [hep-th]].
- [20] E. Herrmann and J. Trnka, “Gravity On-shell Diagrams,” JHEP **11**, 136 (2016) doi:10.1007/JHEP11(2016)136 [[arXiv:1604.03479](#) [hep-th]].
- [21] Z. Bern, E. Herrmann, S. Litsey, J. Stankowicz and J. Trnka, “Evidence for a Nonplanar Amplituhedron,” JHEP **06**, 098 (2016) doi:10.1007/JHEP06(2016)098 [[arXiv:1512.08591](#) [hep-th]].
- [22] C. Cheung, K. Kampf, J. Novotny, C. H. Shen and J. Trnka, “On-Shell Recursion Relations for Effective Field Theories,” Phys. Rev. Lett. **116**, no.4, 041601 (2016) doi:10.1103/PhysRevLett.116.041601 [[arXiv:1509.03309](#) [hep-th]].
- [23] E. Herrmann and J. Trnka, “UV cancellations in gravity loop integrands,” JHEP **02**, 084 (2019) doi:10.1007/JHEP02(2019)084 [[arXiv:1808.10446](#) [hep-th]].
- [24] C. Cheung, K. Kampf, J. Novotny, C. H. Shen, J. Trnka and C. Wen, “Vector Effective Field Theories from Soft Limits,” Phys. Rev. Lett. **120**, no.26, 261602 (2018) doi:10.1103/PhysRevLett.120.261602 [[arXiv:1801.01496](#) [hep-th]].

- [25] J. L. Bourjaily, E. Herrmann and J. Trnka, “Prescriptive Unitarity,” JHEP **06**, 059 (2017) doi:10.1007/JHEP06(2017)059 [[arXiv:1704.05460](#) [hep-th]].
- [26] N. Arkani-Hamed, H. Thomas and J. Trnka, “Unwinding the Amplituhedron in Binary,” JHEP **01**, 016 (2018) doi:10.1007/JHEP01(2018)016 [[arXiv:1704.05069](#) [hep-th]].
- [27] J. L. Bourjaily, E. Herrmann, C. Langer, A. J. McLeod and J. Trnka, “Prescriptive Unitarity for Non-Planar Six-Particle Amplitudes at Two Loops,” JHEP **12**, 073 (2019) doi:10.1007/JHEP12(2019)073 [[arXiv:1909.09131](#) [hep-th]].
- [28] A. Edison, E. Herrmann, J. Parra-Martinez and J. Trnka, “Gravity loop integrands from the ultraviolet,” SciPost Phys. **10**, 016 (2021) doi:10.21468/SciPostPhys.10.1.016 [[arXiv:1909.02003](#) [hep-th]].
- [29] J. L. Bourjaily, E. Herrmann and J. Trnka, “Maximally supersymmetric amplitudes at infinite loop momentum,” Phys. Rev. D **99**, no.6, 066006 (2019) doi:10.1103/PhysRevD.99.066006 [[arXiv:1812.11185](#) [hep-th]].
- [30] N. Arkani-Hamed, C. Langer, A. Yelleshpur Srikant and J. Trnka, “Deep Into the Amplituhedron: Amplitude Singularities at All Loops and Legs,” Phys. Rev. Lett. **122**, no.5, 051601 (2019) doi:10.1103/PhysRevLett.122.051601 [[arXiv:1810.08208](#) [hep-th]].
- [31] J. Trnka, “Towards the Gravituhedron: New Expressions for NMHV Gravity Amplitudes,” [[arXiv:2012.15780](#) [hep-th]].
- [32] E. Herrmann, C. Langer, J. Trnka and M. Zheng, “Positive geometry, local triangulations, and the dual of the Amplituhedron,” JHEP **01**, 035 (2021) doi:10.1007/JHEP01(2021)035 [[arXiv:2009.05607](#) [hep-th]].
- [33] E. Herrmann, C. Langer, J. Trnka and M. Zheng, “Positive Geometries for One-Loop Chiral Octagons,” [[arXiv:2007.12191](#) [hep-th]].
- [34] J. L. Bourjaily, E. Herrmann, C. Langer, A. J. McLeod and J. Trnka, “All-Multiplicity Nonplanar Amplitude Integrands in Maximally Supersymmetric Yang-Mills Theory at Two Loops,” Phys. Rev. Lett. **124**, no.11, 111603 (2020) doi:10.1103/PhysRevLett.124.111603 [[arXiv:1911.09106](#) [hep-th]].
- [35] K. Kampf, J. Novotny, M. Shifman and J. Trnka, “New Soft Theorems for Goldstone Boson Amplitudes,” Phys. Rev. Lett. **124**, no.11, 111601 (2020) doi:10.1103/PhysRevLett.124.111601 [[arXiv:1910.04766](#) [hep-th]].

- [36] J. Tevelev, “Scattering amplitudes of stable curves,” [[arXiv:2007.03831](#) [math.AG]].
- [37] J. L. Bourjaily, E. Gardi, A. J. McLeod and C. Vergu, “All-mass n -gon integrals in n dimensions,” JHEP **08**, no.08, 029 (2020) doi:10.1007/JHEP08(2020)029 [[arXiv:1912.11067](#) [hep-th]].
- [38] J. L. Bourjaily, M. Volk and M. Von Hippel, “Conformally Regulated Direct Integration of the Two-Loop Heptagon Remainder,” JHEP **02**, 095 (2020) doi:10.1007/JHEP02(2020)095 [[arXiv:1912.05690](#) [hep-th]].
- [39] S. L. Devadoss, Tessellations of Moduli Spaces and the Mosaic Operad, arXiv:9807010 [math.AG].
- [40] P. DELIGNE and D. MUMFORD, The irreducibility of the space of curves of given genus, Publications mathématiques de l’I.H.É.S 36 (1969) 75–109.